

## Plastic hinge length of RC columns considering soil-structure interaction

Alireza Mortezaei\*

*Department of Civil Engineering, Semnan Branch, Islamic Azad University, Semnan, Iran*

*(Received February 13, 2013, Revised June 21, 2013, Accepted August 26, 2013)*

**Abstract.** During an earthquake, soils filter and send out the shaking to the building and simultaneously it has the role of bearing the building vibrations and transmitting them back to the ground. In other words, the ground and the building interact with each other. Hence, soil-structure interaction (SSI) is a key parameter that affects the performance of buildings during the earthquakes and is worth to be taken into consideration. Columns are one of the most crucial elements in RC buildings that play an important role in stability of the building and must be able to dissipate energy under seismic loads. Recent earthquakes showed that formation of plastic hinges in columns is still possible as a result of strong ground motion, despite the application of strong column-weak beam concept, as recommended by various design codes. Energy is dissipated through the plastic deformation of specific zones at the end of a member without affecting the rest of the structure. The formation of a plastic hinge in an RC column in regions that experience inelastic actions depends on the column details as well as soil-structure interaction (SSI). In this paper, 854 different scenarios have been analyzed by inelastic time-history analyses to predict the nonlinear behavior of RC columns considering soil-structure interaction (SSI). The effects of axial load, height over depth ratio, main period of soil and structure as well as different characteristics of earthquakes, are evaluated analytically by finite element methods and the results are compared with corresponding experimental data. Findings from this study provide a simple expression to estimate plastic hinge length of RC columns including soil-structure interaction.

**Keywords:** soil-structure interaction; plastic hinge length; nonlinear behaviour; finite element analysis

### 1. Introduction

Following a seismic activity, the ground moves in all directions and each direction of movement gives information about an earthquake. In the past, in analyzing process of building, it was assumed that structural foundation is supported on soil, which is rigid. In the last decades, however, it has been identified that motion at the base of a building is different from the free field (Wolf 1985). This phenomenon that is frequently termed soil-structure interaction (SSI) alters the response characteristics of a structural system.

The effects of SSI on the response of the buildings have been considered as points of interest in earthquake engineering. Several researchers studied the behavior of structures subjected to earthquake under the influence of soil-structure interaction. The inelastic response of rigidly

---

\*Corresponding author, Assistant Professor, E-mail: [a.mortezaei@semnaniau.ac.ir](mailto:a.mortezaei@semnaniau.ac.ir)

supported structures was first studied by Veletsos and Newmark (1960). By using pulse-type excitations and broad-band earthquakes, they derived simple approximate rules for relating the maximum deformation of nonlinear structures to the corresponding values of associated linear structures. Based on the harmonic response of a bilinear hysteretic structure supported on the half-space surface, Bielak (1978) showed that the resonant deformation may be significantly larger than that for rigid supporting soil.

Some examples given by Gazetas and Mylonakis (1998) showed that a number of structures founded on soft soils are vulnerable to SSI. According to available literature, generally, when the shear wave velocity of the supporting soil is less than 600 m/s, the effects of soil-structure interaction on the seismic response of structural systems, particularly for moment resisting building frames, are significant. A research by Eser and Aydemir (2011) revealed that the effects of SSI for yielding systems follow the same general trends observed for elastic systems, although not with the same magnitude. It has been detected that the SSI effects may result in large increments or reductions of the required strengths and expected displacements, with respect to the corresponding fixed-base values. In a more recent study, Ganjavi and Hao (2011) through intensive parametric calculations investigated the effect of SSI on the strength and ductility demands of MDOF systems and RC columns as well as its equivalent SDOF models considering both elastic and inelastic behaviours and concluded that the common SDOF systems might not lead to accurate estimation of the strength and ductility demands of MDOF soil-structure systems, especially for the cases of mid- and high-rise buildings, due to the significant contributions from high vibration modes.

In many seismic design specifications, for example in Iranian Earthquake Code (2005), the effect of soil-structure is disregarded because it is believed that unsafe side errors cannot be introduced in the analytical process. According to the large number of available studies (Tabatabaiefar et al. 2013), it is concluded that SSI affects the dynamic behavior of a soil-structure system in two ways: (1) SSI increases the fundamental natural period of the soil-structure system compared to that of the structure on a rigid base, and (2) SSI modifies the clear damping of the structure. The increase in the natural period results from the flexibility of the supporting soil; while, the change in damping results mainly from the effects of energy dissipation in the soil because of radiation and material damping.

As a result, SSI effects must be incorporated in the performance evaluation of RC buildings such as determination of the elastic seismic loads, estimating the deformations of the building, plastic hinge formation and ductility capacity of structural component. In one hand, plastic hinges are the most severely damaged area of the RC member experiencing large inelastic deformation. Recognising the behaviour and the length of a plastic hinge is not only critical to the deformation capacity design of flexural RC members, but also significant to the retrofit of existing buildings and old structures subjected to severe earthquakes. On the other hand, for designing and specially for detailing of critical regions, a good parameter is the required plastic hinge length. Since, considering the soil-structure interaction may has a significant influence on this parameter, in this paper, different scenarios have been analyzed by inelastic time-history analyses to predict the nonlinear behavior of RC columns considering SSI.

## 2. Research significance

The length over which yielding occurs, i.e. the plastic hinge length, is an important parameter in evaluating the response of reinforced concrete structures and their damage due to seismic loads.

The seismic performance of RC columns is characterized by the inelastic flexural response of the column, the nonlinear behavior of the supporting soil-foundation system and SSI. The responses are also affected by the variability in material properties, structural and foundation lateral stiffness and uncertainty inherent in the seismic ground motions. Previous studies have shown that SSI affects the dynamic behavior of a soil-structure system (Nakhaei and Ghannad 2008). However, all of the works regarding the nonlinear behavior of RC columns were performed on fixed-base columns, i.e. based on a presumed assumption that soil beneath the structure is rigid. The evidence show that neglecting soil-structure interaction lead to serious underestimation of the demand, over-estimation of the capacity (in performance-based design) and thus endanger overall structural safety. For that reason, in this paper, column, foundation and soil were modeled together so that the soil-structure interaction could be taken into account. Firstly, this paper addresses different definitions and estimation techniques concerning plastic hinge length. Then, the key parameters that control the variations on the nonlinear structural response of RC columns are identified due to its interaction with the soil. Finally, findings from this study provide a simple expression to estimate plastic hinge length of RC columns considering soil-structure interaction (SSI).

### 3. Definition of plastic hinge length

Plastic hinges are extension of the ductile design concept, used in building seismically resistant structures. Plastic hinge region is a length of frame element over which flexural yielding is intended to occur due to earthquake design displacements. Energy is dissipated through the plastic deformation of these zones at the end of a member without affecting the rest of the structure. This region involves rebar yielding zone, concrete crushing zone and curvature localization zone. Once, the entire cross section has yielded, it is said to be “plastic”. These plastic hinge regions develop at sections of maximum positive or negative moment and cause a shift in the elastic moment diagram. Once these hinges form, forces redistribute and the usual result is a reduction in the values of maximum negative moments in the support regions and an increase in the values of positive moments between supports which are computed by elastic analysis. Numerous techniques and models are available to estimate the plastic hinge length of RC members as described below.

#### 3.1 Analytical method

The moment-curvature characteristics of a given cross-section can represent the deformation properties of an RC section. As it can be seen from Fig. 1, the schematic moment-curvature curve of an RC member consists of two branches, an ascending branch and a descending branch, and three stages. Typically, point A indicates the cracking point where the concrete starts to crack ( $\phi_{cr}$  and  $M_{cr}$ ). In the initial stages ( $M < M_{cr}$ ), the response is elastic and linear. With an increase in the applied moment, cracking of concrete reduces the flexural rigidity of the section, the extent of which depends on the amount of reinforcement. At the higher load level, corresponding to point B ( $\phi_y$  and  $M_y$ ), the tension steel begins to yield, the concrete cover start spalling and the failure mode of the specimen begins with the formation of a flexural plastic hinge at the base of the column. It is followed by core degradation, and finally by the buckling of longitudinal bars on the compression side. At the point C ( $\phi_u$  and  $M_u$ ), almost all the longitudinal bars buckled and the column failed by the buckling and rupturing of longitudinal bars and the rupturing of transverse bars on the

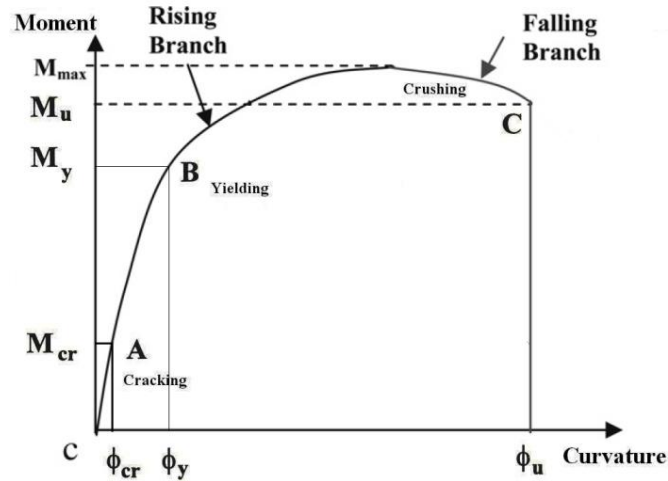


Fig. 1 Qualitative moment-curvature relationship

compression side. A large increase in curvature and ductility normally occurs beyond the yield limit.

Rotation of a member can be determined from curvature distribution along the member length. Based on the conventional structural engineering rules, the rotation (change of slope) between any two points is equal to the area under the curvature diagram between these two points. This is given by

$$\theta_{AB} = \int_A^B \phi \, dx \quad (1)$$

where  $x$  is the distance of element  $dx$  from A. This equation can be applied whether elastic or inelastic curvatures are involved.

The condition at the ultimate load stage of an RC member is shown in Fig. 2. For values of loads smaller than the yield moment,  $M_y$ , the curvature increases gradually from the free end of the member (point A) to the support (point B). There is a large increase in curvature at first yield of the tension steel. At the ultimate load stage, the curvature at the support increases suddenly, so that it causes a large inelastic deformation. Since the concrete between the cracks can carry some tension (tension-stiffening), the curvature fluctuates along the member length. Each of the peaks of curvature corresponds to a crack location. The actual distribution of curvature at the ultimate load level can be idealized into elastic and inelastic (plastic) regions (Fig. 2(c)); thus the total rotation,  $\theta_t$ , over the member length can be divided into elastic,  $\theta_e$ , and plastic,  $\theta_p$ , rotations. The elastic rotation,  $\theta_e$ , (until yielding of steel) can be obtained using the curvature at yield (Eq. (1)). According to Eq. (1), the plastic rotation can be determined, on each side of the critical section, as (Kheyroddin and Mortezaei 2008)

$$\theta_p = \int_0^{l_y} |\phi(x) - \phi_y| \, dx \quad (2)$$

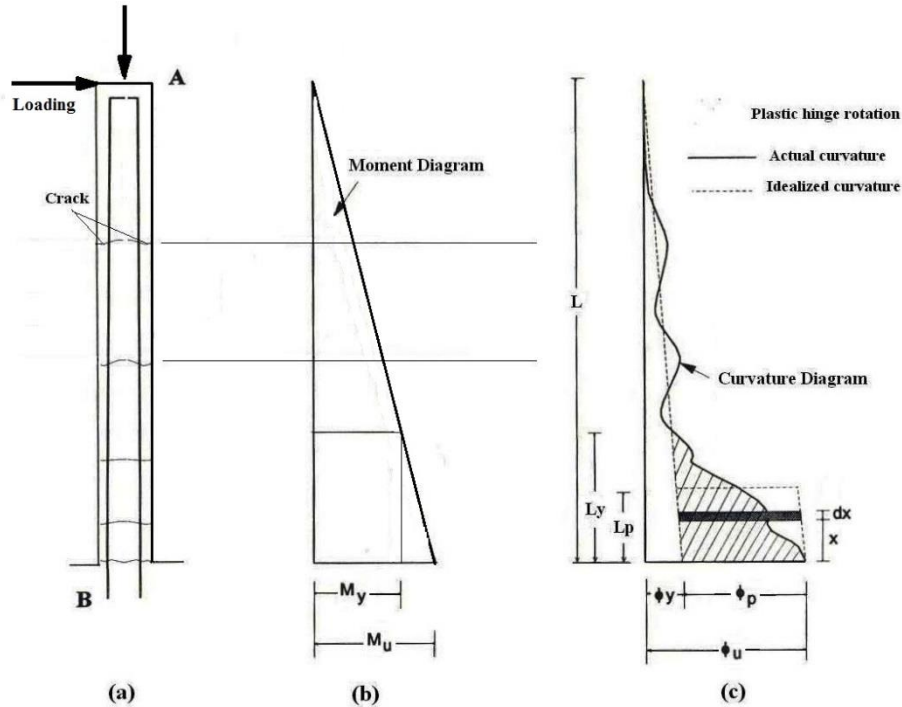


Fig. 2 Schematic curvature distribution along RC member at ultimate stage: (a) RC member, (b) bending moment diagram and (c) curvature diagram

in which  $\phi(x)$  is the curvature at a distance  $x$  from the critical section at the ultimate load stage. The yielding length,  $l_y$ , is defined as the length of the member segment over which the maximum moment exceeds the yield moment,  $M_y$ , or the distance between the critical section and the location where the tension steel first yields (Fig. 2). The shaded area in Fig. 2 is the plastic (inelastic) rotation,  $\theta_p$ , which occurs in addition to the elastic rotation of the plastic hinge at the ultimate load stage. The plastic hinge rotation can be determined either by calculating the size of the shaded area or by an equivalent rectangle of height  $(\phi_u - \phi_y)$  and width  $l_p$ . Using Eq. (2), the equivalent plastic hinge length,  $l_p$ , can be defined as (Kheyroddin and Mortezaei 2008)

$$l_p = \frac{1}{(\phi_u - \phi_y)} \int_0^{l_y} [\phi(x) - \phi_y] dx \quad (3)$$

Therefore, the value of plastic hinge rotation,  $\theta_p$ , at the ultimate stage can be calculated using the following well-known equation

$$\theta_p = (\phi_u - \phi_y) l_p = \phi_p l_p = \beta' \phi_p l_y \quad (4)$$

where  $\phi_u$  and  $\phi_y$  are the curvatures at the ultimate load and yield load, respectively, and  $l_p$  is the equivalent length of the plastic hinge over which the plastic curvature,  $(\phi_p = \phi_u - \phi_y)$ , is assumed to be constant. Eq. (4) results in the same area as the actual plastic curvature distribution (shaded area in Fig. 2(c)). The dimensionless factor,  $\beta'$ , is a shape factor or curvature distribution factor for the

curvature diagram near the support and is less than 1. It may be called a reduction factor applied to the yielding length over which the steel reinforcement yields, so that  $\beta' l_y = l_p$ .

### 3.2 Experimental method

Beam tip displacement test data from reversed cyclic loading of beam-column joint specimens have been used to determine the real plastic hinge lengths (Park and Paulay 1975). From force-displacement and moment-curvature test results, bilinear elastic perfectly plastic models have been used to obtain the yield and ultimate values of  $\phi_y$ ,  $\phi_u$ ,  $\Delta_y$  and  $\Delta_u$ . In order to determine the equivalent bilinear curve for the test results, the area under the curve (force-displacement or moment-curvature) is calculated, and a line having the initial slope of the curve is then drawn through the origin, as shown in Fig. 3. Next, a horizontal line is drawn in a way that the area under the two lines is equal to the area under the original curve. The yield displacement/curvature is then defined as the point of intersection between the two lines and the ultimate value is considered as the maximum value of the displacement/curvature in the inelastic range.

To estimate the flexural deformation capacity, the plastic rotation capacity and the plastic hinge length are used as bellow

$$\theta_p = \frac{\epsilon_{cu} - \epsilon_{ce}}{c} \times l_p \tag{5}$$

Park and Paulay (1975) simplified the curvature distribution along the length of a column using a plastic hinge. Using the second moment area theorem, they calculated the tip displacement of a column. Eqs. (6) and (7) can be solved to determine the value of  $l_p$ .

$$\Delta_p = \Delta_u - \Delta_y \tag{6}$$

$$\Delta_p = (\phi_u - \phi_y) \frac{l_p}{l} \left( 1 - 0.5 \frac{l_p}{l} \right) \tag{7}$$

where  $\Delta_y$  and  $\Delta_u$  represent the yield and the ultimate beam tip displacement from test data, respectively.

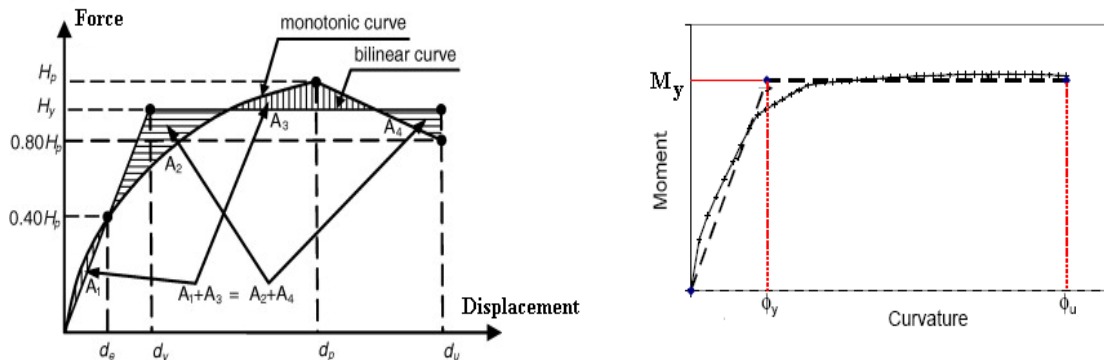


Fig. 3 Equivalent bilinear curve for force-displacement and moment-curvature curve

### 3.3 Empirical method

Empirical equations can also be used to estimate  $l_p$  for RC members. Numerous models are available. Many of these models consider a proportional increase of  $l_p$  with an increase of member length, depth and longitudinal reinforcement dimensions. Comparison of some popular expressions is presented in the next section to estimate the plastic hinge length.

## 4. Past studies

Previous studies in the literature are mainly focused on fixed-base systems, i.e. based on a presumed assumption that soil beneath the structure is rigid, whereas, SSI effects have generally been neglected or underestimated in analysis and design.

The plastic hinge length,  $l_p$ , of RC members depends on a number of parameters, including the definition of yielding and ultimate curvatures, section geometry, material properties, compression and tension reinforcement, transverse reinforcement, cracking and tension-stiffening, the stress-strain curve for the concrete in tension and compression, the stress-strain curve for steel, bond-slip characteristics between concrete and the reinforcing steel, support conditions and the magnitude and type of loading, axial force, width of the loading plate, influence of shear as well as different characteristics of earthquakes. Various expressions have been recommended to be used in  $l_p$  estimations. A comparison of some reported  $l_p$  expressions is provided in Fig. 4, where it can be seen that the analytical value of  $l_p$  is not constant for the different values of the tension reinforcement indices ( $\omega = \rho \cdot f_y / f'_c$ , which  $\rho = A_s / b \cdot d =$  longitudinal reinforcement ratio).

Baker's equation (Baker 1956) gives a constant value of  $l_p$  equal to 194.5 mm (0.77d) for different amounts of reinforcement index ( $\omega$ ). In contrast, in the latest equation proposed by Baker and Amarakone (1964),  $l_p$  increases linearly with the  $c/d$  ratio. Riva and Cohn's formulation (Riva, Cohn 1990) results in the lowest values of plastic hinge length. The methods of Corley (1966), Mattock (1964), and Sawyer (1964) give constant plastic hinge lengths, regardless of the

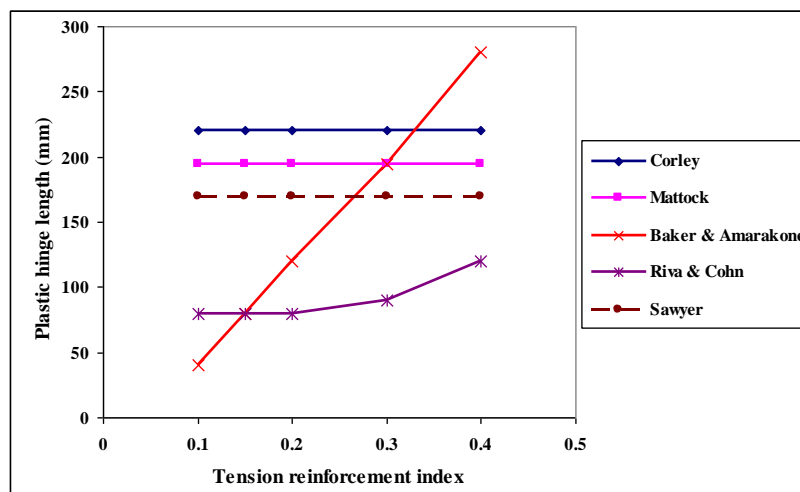


Fig. 4 Comparison of different equations for plastic hinge length

reinforcement index, of 215.4 mm (0.85 d), 196.9 mm (0.78 d), and 168.2 mm (0.66 d), respectively. It is interesting to note that most of the  $l_p$  expressions do not consider axial load as a parameter. More recently, Bae and Bayrak (2008), Mortezaei and Ronagh (2013) and Zhao *et al.* (2011 and 2012) showed that the level of axial load may influence the length of plastic hinges. Specimens tested by Bae and Bayrak (2008) and Zhao (2012) under high axial loads developed longer plastic hinges than those tested under low axial loads. They tested full-scale concrete columns under moderate to high axial load levels and reversed cyclic displacement excursions.

None of the past studies regarding the estimation of plastic hinge length considered soil-structure interaction in their research; whereas, past researches for columns on soil showed that the dynamic interaction between the column and soil have a significant effect on the nonlinear behavior of both of them. Soil-Structure interaction modifies the motion at the base compared to the free-field ground motion, and hence changes the response of the column. Depending on the properties of the column, soil and characteristics of the ground motion, neglecting of SSI may, present false behavior in the column. The realistic earthquake response evaluation of columns, which plastic hinge length is a key parameter of this evaluation, requires consideration of the soil and dynamic interaction effects. Therefore, an investigation into the  $l_p$  of reinforced concrete columns is needed to: 1) reconcile differences encountered in the previous research; and 2) develop an expression that can be used to estimate  $l_p$  more accurately under the ground motions considering soil-structure interaction.

## 5. Soil-structure interaction

Recent earthquakes in Turkey (1999), Taiwan (1999), India (2001), Iran (2003), China (2008), New Zealand (2011) and Japan (2011) provide insight into structural performances and clearly show that soil-structure interaction took place in several structures. The interaction between the structure and the soil during an earthquake is named soil-structure interaction (SSI). This interaction can be generally classified into separate effects: kinematic interaction, inertial interaction, and foundation sliding.

Kinematic interaction is characterized as motion of the structure due to rigid body displacement of the ground surface (Wolf 1985). When the earthquake in the free-field is varying over the area equivalent to that of the rigid foundation, then it can be modified by the rigid foundation. This difference from free field motion is called kinematic interaction between the soil and foundation.

Inertial interaction is distinguished by the motion and deformation of the foundation and structure apart from the motion of the nearby soil. During an earthquake, the ground motion is sent from the soil into the building. The building mass develops an inertia force to resist this change in motion because the rest body has a tendency to remain at rest. This deformation propagates away from the structure in six degrees of freedom of the foundation motion termed as inertial interaction. This removal of energy from the system is referred to as radiation damping in literature.

The sliding of foundation is identified as relative lateral motion between the structural foundation and the adjacent soil. In this paper, first two effects of soil-structure interaction, i.e. kinematic and inertia interaction are considered and the foundation sliding is supposed to be negligible. For modeling of these two characteristics of interaction in time-history analysis, two main categories are existed: direct methods and indirect or multistep methods. In the direct method, the soil and structure are comprised within the same finite element model (Fig. 5) and the boundary conditions are implemented around the soil body and analysis has been done in a single step.

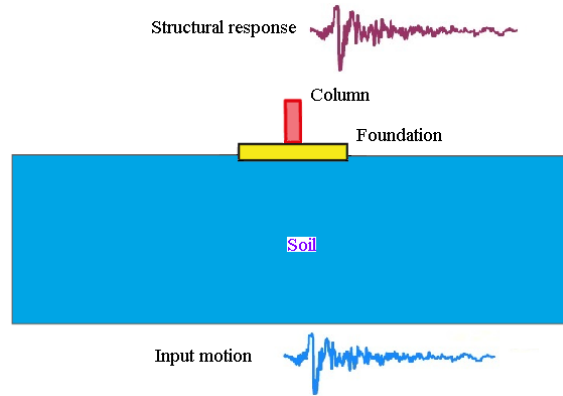


Fig. 5 Modelling of soil-structure system

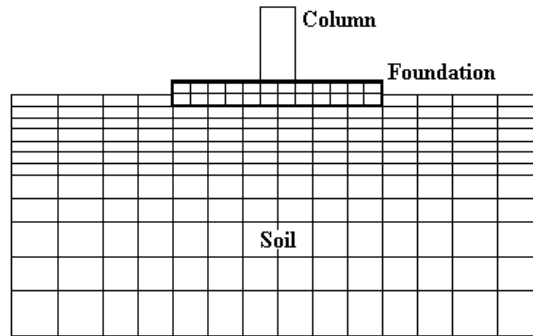


Fig. 6 Finite element meshing for soil and foundation modelling

In this method, which is used in the paper, the response of the system is solving equation of motion of the whole system

$$[M]\{\ddot{u}\} + [K]\{u\} = -[M]\{\ddot{u}_{ff}\} \tag{8}$$

where [M] and [K] are the mass matrix and stiffness matrix of the soil- structure system. In this method, there is a boundary limit obligation and ground accelerations at the bottom of soil domain are applied as input motion. The limitation is that supposed boundaries do not absorb energy. For reducing the effect of reflexive wave, the distance between the structure and the boundaries must be increased. Ghosh and Wilson (1969) concluded that if the distance of the structural centre to the soil finite element model boundaries are within 3–4 times of the foundation radius in horizontal direction and 2–3 times of the foundation radius in the vertical direction, the effects of the reflexive waves are negligible. Hence, the dimensions of the soil field used in the finite element modelling is according to the above research outcomes.

For finite element modelling of soil and foundation, three dimensional quadrilateral elements with 0.5m×0.5m to 2m×2m width have been used (Fig. 6). Horizontal distances between soil boundaries and center of columns have been assumed to be 15 m from each side and vertical distance of soil boundaries have been extended to the bed rock. Bed rock depth has been assumed to be 15 m for all considered soil types.

## 6. Characteristics and database of selected ground motions

The frequency content of earthquake ground motion is an important parameter that affects the dynamic response of structural response. In this paper, the ground motion database compiled for nonlinear time-history (NTH) analyses constitutes a representative number of ground motions from a variety of tectonic environments. A total of 7 records were selected to cover a range of frequency content, duration and amplitude. These records come from earthquakes having a magnitude ( $M_w$ ) range of 6.2 to 7.3. Information pertinent to the ground motion data sets, including station, components of earthquake and peak ground acceleration (PGA) of vertical and horizontal components are presented in Table 1.

The comparison of response spectrum of selected records has been shown in Fig. 7. Utilized in this study is a data processing technique proposed by Iwan et al. (1985) and refined by Iwan and Chen (1994) to recover the long period components from near-fault accelerograms. This process has been elaborated in Boore (2001) and Boore et al. (2002).

Table 1 Selected ground motion database

	Earthquake	Year	Station	Distance (km)	$M_w$	PGA- $H_{max}$ (g)	PGA- $H_{min}$ (g)
1	Gazli (USSR)	1976	Karakyr	5.46	7.1	0.718	0.608
2	Imperial Valley	1979	Bonds Corner	2.68	6.4	0.755	0.588
3	Morgan Hill	1984	Coyote Lake Dam	0.30	6.2	1.298	0.711
4	Erzincan (Turkey)	1992	Erzincan	4.38	6.8	0.515	0.496
5	Landers	1992	Lucerne	2.19	7.3	0.785	0.721
6	Northridge	1994	Rinaldi Rec Stn	6.50	6.7	0.838	0.472
7	Kobe (Japan)	1995	KJMA	0.96	6.9	0.821	0.599

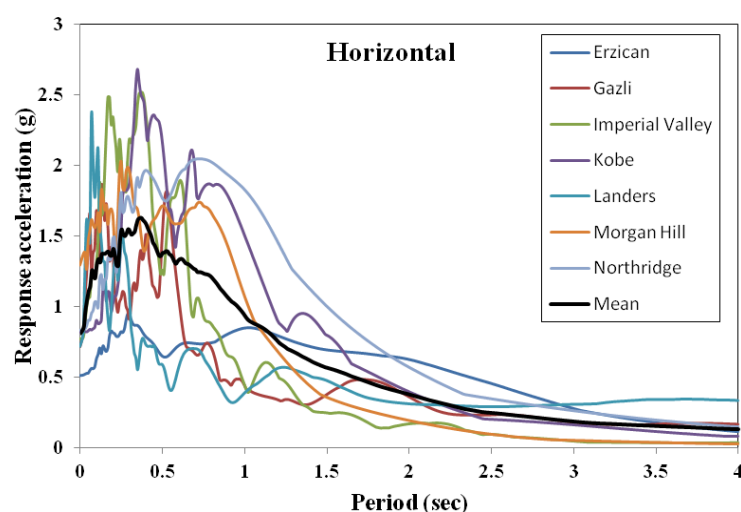


Fig. 7 Response spectrum of horizontal component of selected ground motions

## 7. Verification of analytical models

The capability and accuracy of the finite element program and analytical models in predicting the nonlinear response of RC columns is verified along with a comparison between the analytical and corresponding experimental results. The MISST (Multi-Site Soil-Structure-Foundation Interaction) project was used for evaluating the analytical models (Spencer et al. 2006). This project, that is regarding the bridge testing, is based on Collector-Distributor 36 of the I-10 Santa Monica Freeway that was severely damaged during the Northridge Earthquake in 1994, Fig. 8(b). A 1/2 scale model of the prototype pier was constructed and tested at University of Illinois at Urbana-Champaign (Fig. 9). The diameter of tested specimen was 24 inches with a reinforcement ratio of 3.11% and 0.176% for the longitudinal and transverse directions, respectively. Two earthquake records that were captured during the Northridge earthquake of 1994 were employed during these simulations. The first record was strong motion data collected at the Santa Monica City Hall, which had peak ground acceleration (PGA) of 0.37g. The second record was collected at the Newhall Fire Station and had a PGA of 0.58g. In both cases, the acceleration record was applied along the longitudinal direction of the bridge structure. Ground motions are selected considering various epicentral distances and soil conditions.

Due to the progressive micro-cracking at the interface between the mortar and the aggregates (transition zone), concrete behaves differently under different types and combinations of stress conditions. The propagation of these cracks under the applied loads contributes to the nonlinear behaviour of the concrete. There are many existing concrete constitutive models to simulate cyclic loading effects. The model accepted for this research is a computational constitutive model for concrete subjected to large strains (Vecchio 2000). The FE program is capable of predicting large

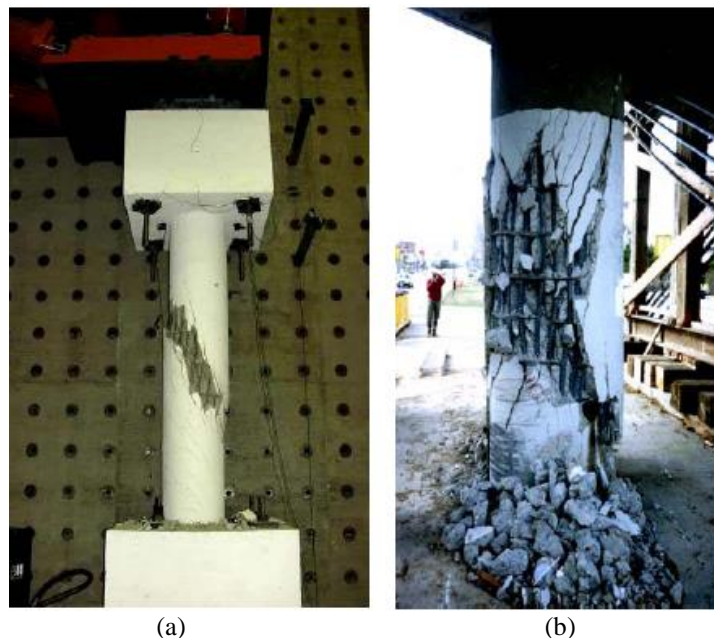


Fig. 8 Behavior of RC tested column under the seismic load: (a) experimental measurement; (b) observed behavior after earthquake

displacement behaviour of structures, taking into accounts both geometric nonlinearities and material inelasticity. The fibre modelling approach has been employed to represent the distribution of material nonlinearity along the length and cross-sectional area of the member. A three-node constant strain triangular elements was used with six degrees of freedom (DOF) and four-node plane stress rectangular elements with eight DOF to model concrete with distributed reinforcement and uses two-node truss bar elements with four DOF to model discrete reinforcement. The interaction between concrete and steel was modelled by a nonlinear spring linkage element for the bond-slip effect. The rebar shares the same nodes at the points of intersection with the shear stirrups (Fig. 10). The meshing of the reinforcement is a special case compared to the volumes. No meshing of reinforcement is needed because individual elements were created in the modeling through the nodes created by the mesh of the concrete volume.



Fig. 9 Experimental setup of the selected RC column

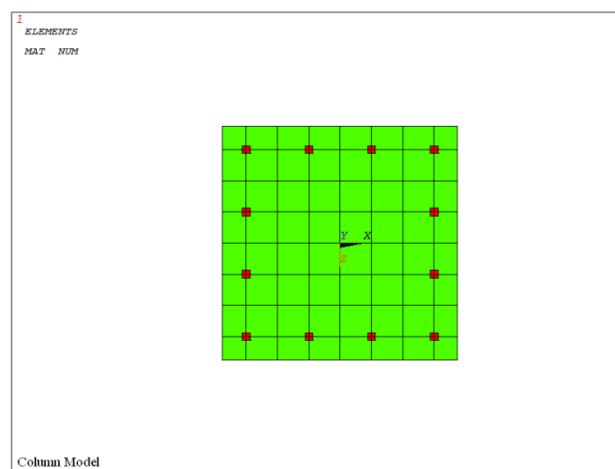


Fig. 10 Column section and meshing in FE program

The goal of the comparison between the finite element model and the experimental work is to ensure that the model including its elements, material properties, real constants and convergence criteria is adequately simulating the response of the member. Fig. 11 presents displacement response histories of RC tested column under 1999 Kobe earthquake. At the terminative times of response history, experimental result is higher than analytical result. This difference may result from shear deformation of tested column.

Load-deformation curve of analytical model is compared with measured values, as shown in Fig. 12. Fig. 12 shows that the FE method can almost exactly follow the measured data. Taking into account of many unknown input parameters, however, this level of accuracy is regarded as acceptable.

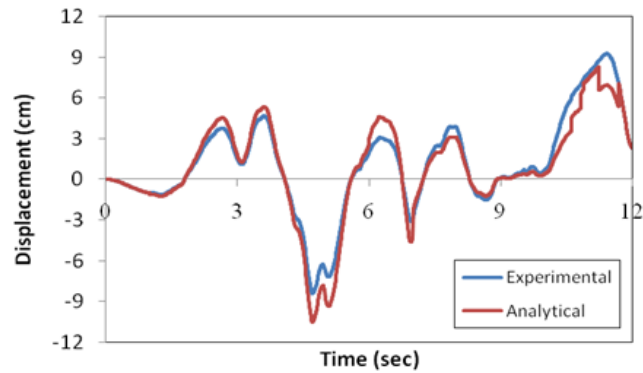


Fig. 11 Lateral displacement history of RC column under seismic excitation

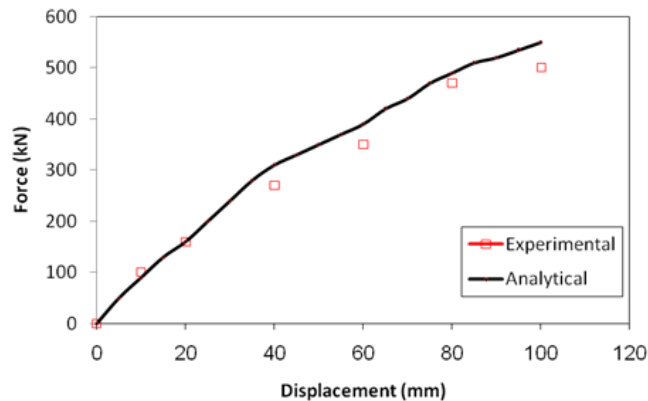


Fig. 12 Load-displacement relationship at the top of column

The failure modes that also obtained from analytical model, are similar to those in the prototype observed following the 1994 Northridge earthquake (Fig. 8(b)). The peak computed lateral force has good agreement with peak measured lateral force. The results indicate that FE program provides reasonable results and as such can be used to approximate the nonlinear behavior of RC columns under dynamic loading.

## 8. Parametric study

In this section, several inelastic time-history analyses have been performed in order to predict the plastic hinge length of RC columns using the FE program. As predicting of the plastic hinge length includes various uncertain input parameters, parameter uncertainty causes uncertainty of the response. Hence, a sensitivity analysis is performed to determine the relative significance of each uncertain variable in the developed computational models on the response measures of columns. In this regard, the so-called tornado diagram, commonly used in decision analysis (Clemen 1996), is employed.

In the tornado analysis, the output variable (plastic hinge length) is assumed to be a known function of a set of input random variables (RVs) whose probability distributions are assumed by the analyst. For each input variable, two extreme values corresponding to predefined upper and lower bounds of its probability distribution are selected. Table 2 presents the random variables used in the sensitivity study. These variables were selected based on preliminary analyses to determine which variables could be excluded. It is to be noted that all variables in Table 2 are defined previously in the text.

Table 2 The parameters used in sensitivity analysis

	Parameter	Notation
1	Axial force	$P$
2	Column height	$H$
3	Soil period	$T$
4	Characteristics of earthquake	$EQ$
5	Longitudinal reinforcement	$A_s$
6	Concrete strength	$f_c$
7	Steel strength	$f_s$
8	Shear wave velocity of soil	$V_s$
9	Yielding curvature	$\phi_y$
10	Ultimate curvature	$\phi_u$

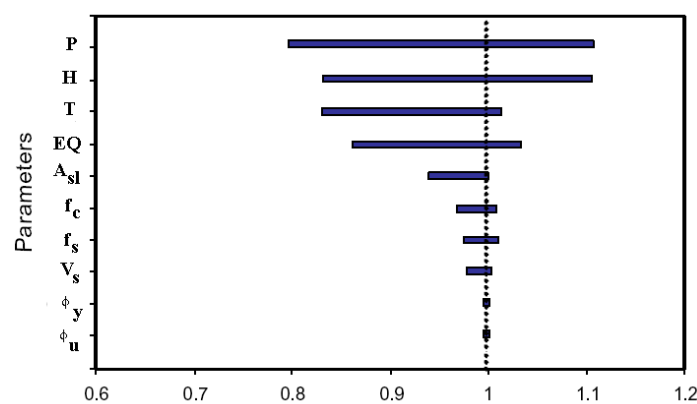


Fig. 13 Sensitivity analyses results for plastic hinge length variation

Fig. 13 shows the results of the sensitivity studies for plastic hinge length. All results are normalized with respect to column dimension. The observations and implications of the tornado diagrams show that, uncertainty in the plastic hinge length is more sensitive to uncertainty in axial load, column geometry, soil period, and characteristics of earthquakes. Changes in the other variables have much smaller effect on the plastic hinge length.

Using the aforementioned method, the influence of various parameters (axial load level ( $P/P_o$ ), height-depth ratio ( $H/h$ ) and soil-structure period ratio) on  $l_p$  are studied under the selected ground motions. In the analysis, the modulus of elasticity (Young's modulus)  $E = 30 \text{ kN/mm}^2$ , Poisson's ratio  $\nu = 0.20$  and the mass density  $\rho = 24 \text{ kN/m}^3$  are assumed in all models. The uni-axial strength for nonlinear modelling of the concrete is considered 250 MPa. The rebar is modeled as steel with yield strength of 400 MPa and an ultimate strength of 600MPa. Eight different soil profiles of single layer with the average shear-wave velocities  $V_s$  of 100 m/sec to 800 m/sec are considered in the analysis. The selected soil profiles are categorized as types 2, 3 and 4 according to classification of the Iranian Earthquake Code (2005). Characteristics of three soil profiles, which have been extracted from the actual geotechnical studies of various projects, are shown in Table 3. Therefore, they have priority over the assumed parameters, which may not be completely conforming to reality.

Table 3 Geotechnical characteristics of some selected soil profiles

Soil type	$V_s$ (m/s)	$E$ (kg/cm <sup>2</sup> )	$G_{\max}$ (kg/cm <sup>2</sup> )	$\rho$ (kg.s <sup>2</sup> /m <sup>4</sup> )	$\nu$
2	600	15900	6250	185	0.29
3	350	5200	1870	179	0.38
4	200	1500	373	155	0.4

## 9. Axial load level

The significant influence of fluctuations in the axial force demand of the columns can be the variation in the shear capacity of the columns. It is well known that the shear capacity of concrete depends on the axial force demand. An increase in the axial force demand in the column such as the one imposed by the vertical components of ground motions results in an increase in the shear capacity of the column which is beneficial to the seismic behavior of the column.

In this regard, to study the effect of axial load on the length of plastic hinge considering soil-structure interaction, 202 nonlinear dynamic analyses are conducted. The square RC columns with various levels of axial load under the 7 selected records are studied. The percentage of longitudinal reinforcements and height over depth ratios are kept constant at 1% ( $\rho_l = 0.01$ ) and 5 ( $H/h=5$ ), respectively. Table 4 and Fig. 14 illustrate the results of the analyses.

For all cases studied in Fig. 14, the length of the plastic hinge is estimated using the procedure described previously. As can be seen in the Figure, the length of the plastic hinge is nearly constant at low axial loads ( $0 < P \leq 0.2P_o$ ). At low axial loads, the obtained  $l_p$  values are equal to  $0.50h$ . Starting at an axial load of approximately  $0.2P_o$ ,  $l_p$  increases with increasing axial loads. The  $l_p$  estimate of  $0.50h$  (Fig. 14) can be compared with  $0.4h$  recommended by Park et al. (1982) and  $0.5h$  recommended by Paulay and Priestley (1992) and  $0.25h$  by Bae and Bayrak (2008). The differences observed in the  $l_p$  estimates can be attributed to the displacement components used to

estimate the  $l_p$  values. Bae and Bayrak (2008) only considered the flexural displacements as the strains experienced by compression bars were obtained from the moment-curvature relationships. It is important to note that in the present paper for the calculation of  $l_p$  not only flexural deformations were considered but also deformations due to bar slip, shear deformations and soil-structure interaction were calculated.

Table 4 Predicted length of plastic hinge for different levels of axial load

Axial Load	Kobe	Northridge	Landers	Erzincan	Morgan Hill	Imperial Valley	Gazli	Average
0	0.48	0.48	0.52	0.48	0.49	0.47	0.48	0.48
0.1	0.49	0.49	0.53	0.5	0.51	0.48	0.47	0.49
0.2	0.56	0.51	0.54	0.51	0.52	0.50	0.59	0.53
0.3	0.74	0.71	0.74	0.75	0.69	0.69	0.73	0.72
0.4	0.87	0.82	0.79	0.99	0.85	1.09	0.89	0.9
0.5	1.04	0.99	1.19	1.20	1.10	1.19	1.19	1.13
0.6	1.31	1.20	1.35	1.37	1.25	1.28	1.33	1.30
0.7	1.49	1.37	1.54	1.55	1.46	1.44	1.48	1.47
0.8	1.74	1.59	1.68	1.70	1.69	1.67	1.65	1.67

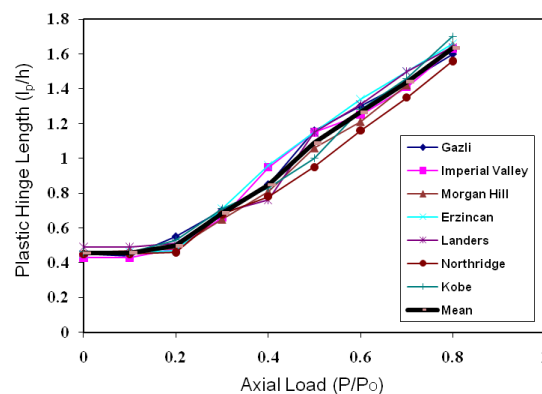


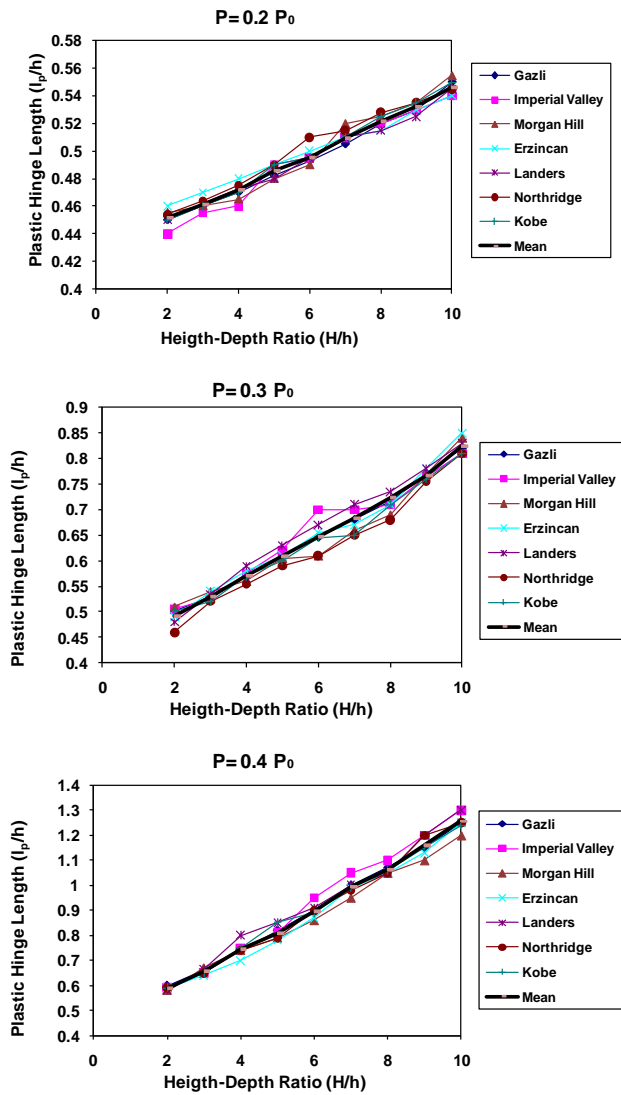
Fig. 14 Relationship between plastic hinge length and axial load

In the Bae and Bayrak experimental tests (2008), the critical section in the columns shifts away from the face of the stub, due to additional confinement effects provided by the stub. Because of the additional confinement provided by the stub to adjacent sections, sections within a distance of approximately  $0.25h$  from the stub remain nearly undamaged. Therefore, in order to estimate the length of the plastic hinge region, (in which columns are expected to dissipate significant amounts of inelastic energy by undergoing large inelastic deformations), Bae and Bayrak suggested subtracting an amount of  $0.25h$  from the overall length in which compressive reinforcing bar strains greater than the yield strain are calculated. Adding the term of  $0.25h$  and considering deformations due to bar slip, shear deformations and soil-structure interaction, Bae and Bayrak's results have been shown to be in good agreement with the experimental tests.

### 10. Height-depth ratio (H/h)

In order to investigate the influence of H/h on the length of plastic hinge, 652 nonlinear dynamic analyses were conducted. The square RC columns with various levels of axial loads and height over depth ratios subjected to the 7 selected records were studied. At this stage of the parametric study, the longitudinal reinforcement ratio was kept constant at  $\rho_l = 0.01$ . The results of the analyses are summarized in Figs. 15 and 16.

Bearing in mind the Zhao works (2012) and adding the term of 0.25h to the Bae and Bayrak experimental tests (2008) and considering deformations resulting from bar slip, shear deformations and soil-structure interaction helps in realizing a good agreement with the experimental tests.



Continued

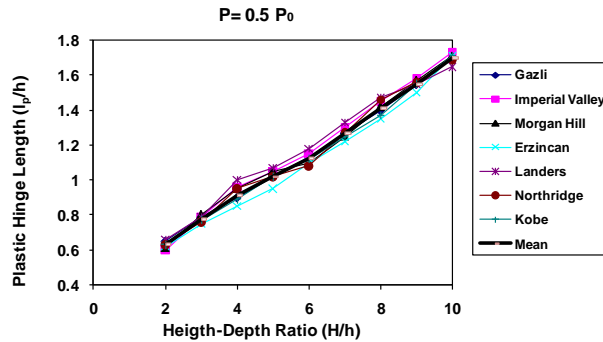


Fig. 15 Relationship between plastic hinge length and height-depth ratio for various levels of axial load

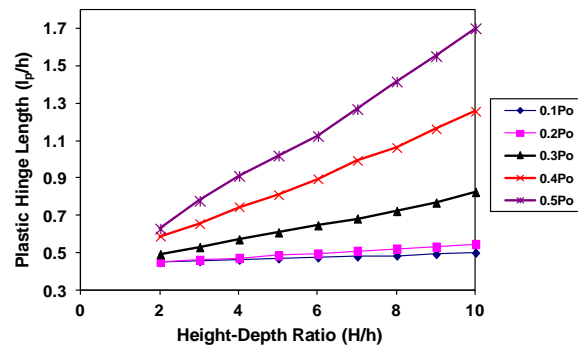


Fig. 16 Relationship between plastic hinge length (average) and height-depth ratio for various levels of axial load

As is seen in Fig. 16,  $l_p$  increases as  $H/h$  increases for a given axial load level. At low axial loads ( $\approx 0.2P_0$ ), the increases observed in  $l_p$  with increasing  $H/h$  are insignificant. For a given  $H/h$ , the  $l_p$  increases as axial loads increase. The increases in  $l_p$  observed at small  $H/h$  ( $2 < H/h < 3$ ) are less pronounced than those observed at large  $H/h$  values. The comparison between results in this study and past studies show that plastic hinge length in RC columns considering soil-structure interaction is lower than plastic hinge length in RC columns subjected to far- and near-fault ground motions on fixed base (Mortezaei and Ronagh 2013).

## 11. Proposed expression for plastic hinge length

Several factors influence the length of plastic hinge, such as: 1) level of axial load; 2) moment gradient; 3) the value of shear stress in the plastic hinge region; 4) the amount and mechanical properties of longitudinal and transverse reinforcement; 5) strength of concrete; 6) level of confinement provided in the potential plastic hinge zone; 7) different characteristics of earthquakes; and 8) soil-structure interaction. The simplified equations available in the literature do not contain all, or even most, of the aforementioned factors. Hence, large variations exist in the values of plastic hinge length calculated using these empirical equations, as shown clearly in Fig. 4.

Baker, in his work, considered most of the parameters affecting plastic hinge length. He found that the contribution of the longitudinal reinforcement effect is not considerable. Bae and Bayrak (2008) presented an expression for the estimation of plastic hinge length of RC columns. Compared to other equations presented by other researchers, this equation includes the level of axial force ( $P/P_0$ ) and height over depth ratio ( $H/h$ ). However, this equation presents a problem, in that only flexural displacements were considered in the proposed analysis. For simplicity of proposed equation, a linear relationship between considered parameters is supposed. Using the results of different scenarios that have been obtained by inelastic time-history analyses, least squares analyses were performed to determine a coefficient for each parameter. Based on the obtained coefficients from the least squares analyses, following equations are suggested for the estimation of plastic hinge length in RC columns under the earthquake loading considering soil-structure interaction:

$$\frac{l_p}{h} = 0.80 \left[ 1 + 0.40 \frac{P}{P_0} \right] \left( \frac{H}{h} \right)^{0.2} k \quad \text{for } P/P_0 > 0.2 \quad (9)$$

$$\frac{l_p}{h} = 0.50 \quad \text{for } 0 < P/P_0 \leq 0.2$$

In the above,  $k = 0.50$  when  $T_s/T \geq 1.0$ ; and  $k = 1.0$  when  $T_s/T \leq 0.5$  and  $k = (0.5 - T_s/T) + 1$ , where  $0.5 < T_s/T < 1$ , which  $T_s$  is soil period and  $T$  the main period of building.

These equations are compared favourably with the calculated values in this paper and measured values reported in the MISST (Spencer et al. 2006) project and Bae and Bayrak (2008) and Zhao (2012) experimental works. To investigate the accuracy of above equations, the plastic hinge length of four RC columns specimens that were tested by MISST (Spencer et al. 2006) project, are estimated using various expressions and compared with the measured plastic hinge length in Table 3.

The result of the comparison shows that by means of the proposed equations, reasonable estimations can be made of the plastic hinge length of RC columns under the high and low axial load levels considering soil-structure interaction. Also, the result of comparison of proposed equations and some past equations show that using some equations may overestimate the plastic hinge length of RC columns and vice versa; but the proposed equations can calculate the plastic hinge length of RC columns reasonably, in both high level and low level of axial load.

Table 5 Estimated plastic hinge length by various expressions

Specimen	Baker	Corley	Mattock	Park et al.	Paulay & Priestley	Sheikh & Khoury	Measured	Proposed equation
Case 1	0.57h	0.49h	0.70h	0.40h	0.80h	1.00h	0.98h	1.00h
Case 2	0.62h	0.52h	0.80h	0.40h	0.96h	1.00h	1.07h	1.13h
Case 3	0.60h	0.49h	0.70h	0.40h	0.72h	1.00h	0.61h	0.65h
Case 4	0.52h	0.49h	0.70h	0.40h	0.72h	1.00h	0.59h	0.64h

A comparison on  $l_p$  has also been done among some code specifications, as shown in Table 6. As the results show, except Hon Kong code of practice for concrete (2004) and Canadian concrete

code (2004), potential length of plastic hinge specified by other codes is not satisfactory for columns carrying high axial load and can be non-conservative in some cases.

Table 6 Comparison of plastic hinge length among some code specifications

Code		Plastic hinge length
1	ACI 318-08	largest of (a) 1/6 of the clear span of the column; (b) Maximum cross-sectional dimension of the column; (c) 18 in. (457 mm)
2	CSA23.3-04	The plastic hinge length shall be determined as follows: (a) where $P_f \leq 0.5\phi_c f'_c A_g$ , the length shall be not less than 1.5 times the largest member cross-section dimension or one-sixth of the clear span of the member; (b) where $P_f > 0.5\phi_c f'_c A_g$ , the length shall be not less than twice the largest member cross-section dimension or one-sixth of the clear span of the member.
3	Indian Standard	Length shall not be less than the largest of (a) one-sixth of the clear span of the column; (b) maximum cross-sectional dimension of the column; (c) 450 mm.
4	Iranian Concrete Code (ICC)	Length shall not be less than the largest of (a) overall depth of a column, (b) 1/6 of the clear height of a column (c) 450 mm
5	Hong Kong Code of Practice for Structural Use of Concrete 2004	(a) For $0 < N/(A_g f_{cu}) \leq 0.1$ , the extent of critical region is taken as 1.0 times the greater dimension of the cross-section or where the moment exceeds 0.85 of the maximum moment, whichever is larger; (b) For $0.1 < N/(A_g f_{cu}) \leq 0.3$ , the extent of critical region is taken as 1.5 times the greater dimension of the cross-section or where the moment exceeds 0.75 of the maximum moment, whichever is larger; and (c) For $0.3 < N/(A_g f_{cu}) \leq 0.6$ , the extent of critical region is taken as 2.0 times the greater dimension of the cross-section or where the moment exceeds 0.65 of the maximum moment, whichever is larger.
6	Building Standard Law of Japan	$L_p = 0.2L - 0.1h$

## 12. Conclusions

Conventionally, in earthquake engineering, it has been common to assume that soil-structure interaction (SSI) is useful during an earthquake. As a result, it has become common practice to avoid the difficulty of considering SSI by simply ignoring its effects. Whereas, the variations in

structural dynamic properties due to soil-structure can lead to higher inertia forces depending on the period of building, damping levels and ductility factor. Therefore, even if soil-structure interaction induces dampening, it can also cause increased displacement in the overall structure. Due to this possibly detrimental effect, it is necessary to take soil-structure interaction into consideration during analysis.

Plastic hinge region is a length of frame element over which flexural yielding is intended to occur due to earthquake design displacements. Plastic hinges form at the maximum moment regions of RC columns. The determination of the length of plastic hinge is a critical step in predicting the lateral load versus drift response of columns. As it is difficult to estimate the plastic hinge length using analytical methods, it is often estimated based on experimental data or empirical equations. This paper presents the results of a comprehensive analytical study on the length of plastic hinge in RC columns considering soil-structure interaction. Hundreds of time-history analyses have been performed in order to evaluate the plastic hinge lengths, and the results are presented. The following conclusions can be drawn based on the results:

1. The analytical results show good correlation with the available experimental results and indicate the usefulness of the nonlinear finite element as a powerful tool to study the behaviour of different types of RC elements subjected to dynamic loading considering soil-structure interaction.
2. The above mentioned method of calculating the plastic hinge length gives good correlation with the experimental values.
3. The results show that potential  $l_p$  specified by some code is not satisfactory for columns supporting high axial loads and can even be non-conservative in some cases.
4. Analytical models for columns analysed under high axial loads exhibit longer plastic hinges than those analysed under low axial loads.
5. The results show that the effect of soil-structure interaction on both structural and soil performance is worth to be taken into consideration not only for special type of structures but also for common structure for which the response values can be different from the decoupled analyses results.
6. The seismic performance of analyzed RC columns during selected earthquake records show that properly designed RC columns and estimated plastic hinge length are capable of carrying on large ground motion with little or no damage.
7. The following equations, developed in this research, provide a further insight into the understanding of the plastic hinge length of RC members and allow a better estimation of the plastic hinge length of RC columns subjected to the earthquake loading considering soil-structure interaction:

$$\frac{l_p}{h} = 0.80 \left[ 1 + 0.40 \frac{P}{P_0} \right] \left( \frac{H}{h} \right)^{0.2} k \quad \text{for } P/P_0 > 0.2$$

$$\frac{l_p}{h} = 0.50 \quad \text{for } 0 < P/P_0 \leq 0.2$$

## References

- American Concrete Institute (2008), *Building Code Requirements for Structural Concrete (ACI 318-08) and Commentary (ACI 318R-08)*, Farmington Hills, MI.

- Bae, S. and Bayrak, O. (2008), "Plastic hinge length of reinforced concrete columns", *ACI Struct. J.*, **105**(3), 290-300.
- Baker, A.L.L. (1956), *Ultimate load theory applied to the design of reinforced and prestressed concrete frames*, Concrete Publications Ltd., London, UK, 91.
- Baker, A.L.L. and Amarakone, A.M.N. (1964), "Inelastic hyper-static frame analysis", *Flexural Mechanics of Reinforced Concrete*, SP-12, American Concrete Institute, Farmington Hills, MI, 85-142.
- Bielak, J. (1978), "Dynamic response of non-linear building-foundation systems", *Earthq. Eng. Struct. Dyn.*, **6**, 17-30.
- Boore, D. (2001), "Effect of baseline correction on displacements and response spectra for several recordings of the 1999 Chi-Chi, Taiwan, earthquake", *B. Seismol. Soc. Am.*, **91**(5), 1199-1211.
- Boore, D., Stephens, C.D. and Joyner, W.B. (2002), "Comments on baseline correction of digital strong motion data: Examples from the 1999 Hector Mine California earthquake", *B. Seismol. Soc. Am.*, **92**(4), 1543-1560.
- Clemen, R.T. (1996), *Making hard decisions: an introduction to decision analysis*, 2nd ed. Belmont, CA, Duxbury, 688.
- Code of Practice for Structural Use of Concrete (2004), Second edition, Buildings Department, The Government of the Hong Kong Special Administrative Region, Kowloon Hong Kong.
- Corley, W.G. (1966), "Rotational capacity of reinforced concrete beams", *J. Struct. Div.- ASCE*, **92**(ST5), 121-146.
- CSA Committee A23.3-04 (2004), *Design of concrete structures: structures (design) – a national standard of Canada*, Canadian Standards Association, Rexdale, Canada, 240.
- Eser, M. and Aydemir, C. (2011), "The effect of soil-structure interaction on inelastic displacement ratio of structures", *Struct. Eng. Mech.*, **39**(5), 683-702.
- Gazetas, G. and Mylonakis, G. (1998), "Seismic soil-structure interaction: new evidence and emerging issues", *Geotechnical Special Publication No. 75*, ASCE, Reston, Va., 1119-1174.
- Ganjavi, B. and Hao, H. (2011), "Elastic and inelastic response of single- and multi-degree-of-freedom systems considering soil structure interaction effects", *Australian Earthquake Engineering Society Conference*, Australia, NA, pp. NA.
- Ghosh, S. and Wilson, E.L. (1969), "Dynamic stress analysis of axi-symmetric structures under arbitrary loading", Report no. EERC 69-10, University of California, Berkeley.
- Indian Standard for Plain and Reinforced Concrete Code of Practice (2000), Bureau of Indian Standards, New Delhi-110002.
- Iranian Code of Practice for Seismic Resistant Design of Buildings (3rd Edition), Standard No. 2800-05, Building and Housing Research Center of Iran (BHRC).
- Iranian Code of Practice for Seismic Resistant Design of Buildings (2005), Chapter 9, Building and Housing Research Centre, Tehran, Iran.
- Iwan, W.D., Moser, M.A. and Peng, C.Y. (1985), "Some observations on strong-motion earthquake measurements using a digital accelerograph", *B. Seismol. Soc. Am.*, **75**, 1225-1246.
- Iwan, W.D. and Chen, X.D. (1994), "Important near-field ground motion data from the landers earthquake", *Proceedings of the 10th European Conference on Earthquake Engineering*, Vienna, Austria.
- Kheyroddin, A. and Mortezaei, A. (2008), "The effect of element size and plastic hinge characteristics on nonlinear analysis of RC frames", *Iranian J. Sci. Technol. B*, **32**(B5), 451-470.
- Mattock, A.H. (1964), "Rotational capacity of hinging regions in reinforced concrete beams", *Flexural Mechanics of Reinforced Concrete*, SP-12, American Concrete Institute, Farmington Hills, MI, 143-181.
- Mortezaei, A. and Ronagh, H.R. (2013), "Plastic hinge length of reinforced concrete columns subjected to both far-fault and near-fault ground motions having forward directivity", *Struct. Des.Tall Spec.*, **22**(12), 903-926.
- Nakhaei, M. and Ghannad, M.A. (2008), "The effect of soil-structure interaction on damage index of buildings", *Eng. Struct.*, 1491-1499.
- Park, R. and Paulay, T. (1975), *Reinforced concrete structures*, New York, John Wiley & Sons Inc, 769.

- Park, R., Priestley, M.J.N. and Gill, W.D. (1982), "Ductility of square-confined concrete columns", *J. Struct. Div.- ASCE*, **108**(ST4), 929-950.
- Paulay, T. and Priestley, M.J.N. (1992), *Seismic design of reinforced concrete and masonry buildings*, John Wiley and Sons, New York, 767.
- Riva, P. and Cohn, M.Z. (1990), "Engineering approach to nonlinear analysis of concrete structures", *J. Struct. Div. - ASCE*, **116**, 2162-2186.
- Sawyer, H.A. (1964), "Design of concrete frames for two failure stages", *Proceedings of international symposium on the flexural mechanics of reinforced concrete*, Miami, ACI SP-12,405-431.
- Spencer Jr., B.F., Elnashai, A., Kuchma, D., Kim, S., Holub, C. and Nakata, N. (2006), *Multi-Site Soil-Structure-Foundation Interaction Test (MISST)*, University of Illinois at Urbana-Champaign.
- Tabatabaiefar, S.H.R., Fatahi, B. and Samali, B. (2013), "Lateral seismic response of building frames considering dynamic soil-structure interaction effects", *Struct. Eng. Mech.*, **45**(3), 311-321.
- The Building Standard Law of Japan, on CD-ROM (2011), Building Guidance Division, Housing Bureau, Ministry of Land, Infrastructure and Transport, Japan, 237.
- Vecchio, F.J. (2000), "Disturbed stress field model for reinforced concrete: formulation", *J. Struct. Eng.-ASCE*, **126**(9), 1070-1077.
- Veletsos, A.S. and Newmark, N.M. (1960), "Effect of inelastic behavior on the response of simple systems to earthquake motions", *Proc., 2nd World Conf. Earthquake Engineering*, 895-912.
- Wolf, J.P. (1985), *Dynamic soil-structure interaction*, Englewood Cliffs, NJ, Prentice-Hall, USA.
- Zhao, X. (2012), "Investigation of plastic hinges in reinforced concrete (RC) structures by finite element method and experimental study", Department of Civil and Architectural Engineering, City University of Hong Kong, Hong Kong, 293.
- Zhao, X., Wu, Y.F, Leung, A.Y.T. and Lam, H.F. (2011), "Plastic hinge length in reinforced concrete flexural members", *Procedia Eng.*, **14**, 1266-1274.
- Zhao, X., Wu, Y.F and Leung, A.Y.T. (2012), "Analysis of plastic hinge regions in reinforced concrete beams under monotonic loading", *Eng. Struct.*, **34**, 466-482.

## Notations

$A_g$  = gross area of section  
 $A_s$  = area of tension reinforcement  
 $b$  = width of compression face of member  
 $c$  = distance from extreme compression fiber to neutral axis  
 $d$  = effective depth of beam  
 $EQ$  = characteristics of earthquake  
 $f_c$  = compressive strength of concrete  
 $f'_c$  = compressive strength of concrete  
 $f_{cu}$  = characteristic compressive strength of concrete  
 $f_y$  = yield stress of reinforcement  
 $f_s$  = yield stress of reinforcement  
 $h$  = overall depth of column  
 $H$  = distance from critical section to point of contraflexure  
 $L$  = column height  
 $l_p$  = plastic hinge length  
 $M_{cr}$  = bending moment at cracking  
 $M_y$  = bending moment at yield  
 $M_u$  = bending moment at ultimate  
 $M_w$  = earthquake magnitude  
 $N$  = design ultimate axial force  
 $P$  = applied axial force  
 $P_o$  = nominal axial load capacity  
 $P_f$  = factored axial load  
 $V_s$  = shear wave velocity  
 $\Delta u$  = ultimate displacement  
 $\Delta y$  = yield displacement  
 $\epsilon_{ce}$  = elastic concrete compressive strain  
 $\epsilon_{cu}$  = maximum concrete compressive strain  
 $\phi$  = curvature  
 $\phi_{cr}$  = cracking curvature  
 $\phi_y$  = yield curvature  
 $\phi_u$  = ultimate curvature  
 $\phi_c$  = resistance factor for concrete  
 $\theta$  = rotation  
 $\theta_e$  = elastic rotation  
 $\theta_p$  = plastic rotation  
 $\theta_t$  = total rotation  
 $\rho_l$  = longitudinal reinforcement ratio  
 $\rho$  = mass density  
 $E$  = modulus of elasticity  
 $\nu$  = poisson's ratio  
 $T_s$  = soil period